AD-A266 120 ON PAGE

Form Approved
OBM No. 0704-0188

1. Agency Use Only *(Leave blank).*	2. Report Date. December1992	3. Report Type and Dates Covered. Final - Journal Article

4. Title and Subtitle.
Strong resonance features present in the acoustic signatures of submerged elastic structures

5. Funding Numbers.
Program Element No 0601153N
Project No. 3202
Task No. 350
Accession No. DN255011
Work Unit No 12211B

6. Author(s).
Michael F. Werby and Gulliermo C. Gaunaurd*

7. Performing Organization Name(s) and Address(es).
Naval Research Laboratory
Acoustics Division
Stennis Space Center, MS 39529-5004

8. Performing Organization Report Number.
JA 221:066:91

9. Sponsoring/Monitoring Agency Name(s) and Address(es).
Naval Research Laboratory
Basic Research Management Office
Stennis Space Center, MS 39529-5004

10. Sponsoring/Monitoring Agency Report Number.
JA 221:066:91

11. Supplementary Notes.
Published in Optical Engineering.
*Naval Surface Warfare Center, Silver Spring, MD 20903-5000

12a. Distribution/Availability Statement.
Approved for public release; distribution is unlimited.

12b. Distribution Code.

13. Abstract *(Maximum 200 words).*

Acoustic signals scattered from submerged elastic targets have produced interesting backscattered signals in the appropriate frequency region particularly because of the presence of resonances. Considerable work has been done for spherically and cylindrically shaped objects out to moderate frequencies for both solids and shells. Only recently, however, have researchers reported results for elongated objects such as spheroidal solids and shells. Further, the higher-frequency region for spheres has not been investigated extensively. A series of calculations that are characteristic of elongated targets or of spherical shells in the higher-frequency region are reported. Some of the discussed results involve bending resonances caused by obliquely incident plane waves on elongated objects and their relation to flexural resonances of beams; classes of resonances that are related to waves creeping along the longest and shortest meridians of a spheroid: flexural resonances A_o resonances) for shells in the time domain near the coincidence frequency; and high-frequency thickness effects when scattering from shells, and their prediction based on flat plate theory. Several numerical examples are shown.

14. Subject Terms.
Acoustic scattering, shallow water, waveguide propagation

15. Number of Pages.
10

16. Price Code.

17. Security Classification of Report.	18. Security Classification of This Page.	19. Security Classification of Abstract.	20. Limitation of Abstract.
Unclassified	Unclassified	Unclassified	SAR

DISCLAIMER NOTICE

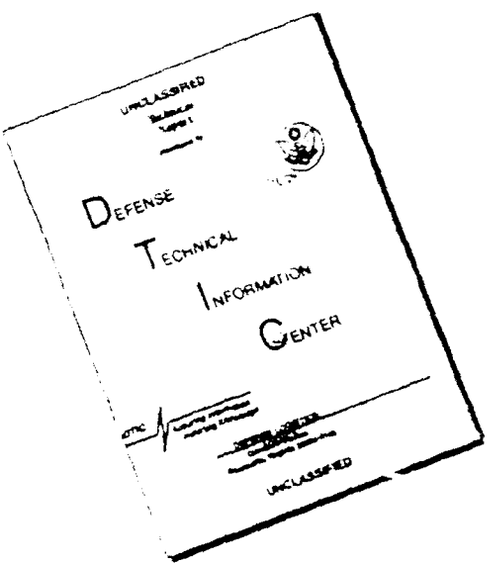

THIS DOCUMENT IS BEST QUALITY AVAILABLE. THE COPY FURNISHED TO DTIC CONTAINED A SIGNIFICANT NUMBER OF PAGES WHICH DO NOT REPRODUCE LEGIBLY.

Strong resonance features present in the acoustic signatures of submerged elastic structures

Michael F. Werby
Naval Oceanographic and Atmospheric Research Laboratory
Code 221
Bay St. Louis, Mississippi 39529-5004

Guillermo C. Gaunaurd
Naval Surface Warfare Center
Dahlgren Division, White Oak Detachment
Research Department, Code R-42
Silver Spring, Maryland 20903-5000

Abstract. *Acoustic signals scattered from submerged elastic targets have produced interesting backscattered signals in the appropriate frequency region particularly because of the presence of resonances. Considerable work has been done for spherically and cylindrically shaped objects out to moderate frequencies for both solids and shells. Only recently, however, have researchers reported results for elongated objects such as spheroidal solids and shells. Further, the higher-frequency region for spheres has not been investigated extensively. A series of calculations that are characteristic of elongated targets or of spherical shells in the higher-frequency region are reported. Some of the discussed results involve bending resonances caused by obliquely incident plane waves on elongated objects and their relation to flexural resonances of beams, classes of resonances that are related to waves creeping along the longest and shortest meridians of a spheroid: flexural resonances (A_0 resonances) for shells in the time domain near the coincidence frequency, and high-frequency thickness effects when scattering from shells, and their prediction based on flat plate theory. Several numerical examples are shown.*

Subject terms: automatic target recognition; acoustic scattering; echo-signatures; submerged shells; resonance scattering; thickness resonances

Optical Engineering 31(12), 2562-2571 (December 1992)

1 Introduction

Resonances are pervasive and occur in all areas of the physical, engineering, and biological sciences. They are characterized by the fact that they occur at discrete frequency values, and when they occur, a characteristic event takes place. This event can be complicated and difficult to distinguish from other physical mechanisms unrelated to resonances, but they are usually distinguishable and can be related to a particular process. Our interest in this paper is to investigate particularly large and distinguishable resonances that manifest themselves in both the frequency and time domains. In the acoustics literature, three main classes of resonances have been studied.[1-17] These are Lamb resonances for shells and Rayleigh resonances and whispering gallery resonances for solids. These resonances are not particularly pronounced, and in this work we examine classes of resonances that are more pronounced in magnitude or pattern in either the time or frequency domains. In the next section we examine some useful theoretical considerations and then go on to examples of (1) flexural or bending resonances caused by plane oblique incident waves on a spheroid, (2) resonances at the coincidence frequency (the frequency at which the phase speed of the flexural Lamb wave equals the speed of sound in the fluid) on elastic shells, and (3) thickness "resonances" caused by high-frequency incident plane waves on a submerged elastic shell. Each of these classes of resonances is rather large, has characteristic curves, and has locations that can be predicted using simplified expressions.

2 Theoretical Considerations

2.1 *Rayleigh, Lamb, and Flexural Resonances*

We briefly discuss flexural or bending resonances excited on a spheroid, and for contrast the more well known resonances caused by the generation of Rayleigh waves on an elastic solid and Lamb waves on elastic shells. More detailed discussions were presented in two other papers.[15,17] Rayleigh, or rather leaky-Rayleigh-type, resonances are generated when incident plane waves impinge on fluid-loaded elastic solids of rotation such as spheres and spheroids. They correspond to frequencies at which the Rayleigh waves have half-integral wavelengths on the object surface (this does not preclude interior contributions of the waves), thus producing standing waves on the surface, which in turn radiate back into the fluid. The extended boundary condition (EBC) method[1-9] offers the possibility for predicting such resonances (see Ref. 17). Lamb resonances are the analog for shells in which it is possible to excite both symmetric (extensional) and antisymmetric (flexural) resonances.[10,11] The bending or flexural resonances (flexurals in this context are not to be confused with antisymmetric Lamb modes) occur on elongated objects such as spheroids both for solids and shells and can be modeled using the approximate theory of beams due to Timoshenko.[12]

Paper ATR-02 received Feb. 25, 1992; accepted for publication June 29, 1992.

2.2 Resonance Scattering Theory—Time Domain

The partial wave series that emerges from normal mode theory for separable geometries can be represented in distinct partial waves or modes. It has been shown that a representation due to a distinct mode n can be written in the Breit-Wigner form[12]:

$$f_n(x) = \frac{2}{x}\exp[2i\xi_n^{(r)}]\left\{\frac{-\left(\frac{1}{2}\right)\Gamma_n^{(r)}}{x - x_n^{(r)} + \left(\frac{1}{2}\right)\Gamma_n^{(r)}} + \exp[-i\xi_n^{(r)}]\sin\xi_n^{(r)}\right\} \quad (1)$$

where $x = ka$ and $x_n^{(r)}$ is the n'th mode, $(\frac{1}{2})\Gamma_n^{(r)}$ is the resonance half-width, and where

$$\exp[2i\xi_n^{(r)}] = -\frac{h_n^{(2)}(x)}{h_n^{(1)}(x)}$$

Here we have absorbed the $(2n-1)$ factor into the expansion coefficient. Equation (1) is here implicitly understood to apply for the $l=1$ resonance contained within the n'th mode. This form is of interest because it shows that a modal contribution can be represented in terms of an acoustical background as well as the resonance contribution. Note that this form of a resonance occurs in many branches of physics and engineering. This representation presents the resonances in a manner such that the resonant part (the first term in the braces) is clearly separate from the potential part (the second term). Further, it shows explicitly the half-width as well as the frequency of the resonances. The form of Eq. (1) also proves useful because we use residue theory to Fourier transform this equation to the time domain.

We consider two incident waveforms (see Refs. 18 through 21), one a delta function in time, which gives a continuous and constant (cw) frequency spectrum, and the other a pulse which is sufficiently localized in time that we are able to isolate individual events in the scattered signal. Specifically,

$$P_- = \cos(\omega_0 t)\exp[-\alpha t^2] = \cos(ka_0 s)\exp[-\alpha s^2] \quad (2)$$

where $s = ct/a$, $k = 2\pi/\lambda$, and where s is a reduced time variable and k is the incident wavenumber. Here we refer to ω_0 as the carrier frequency. The scattered signal in the time domain is

$$g_i(ka) = \int_{s=-\infty}^{s=\infty}\exp(ikas)\cos(ka_0 s)\exp[-\alpha s^2]\,ds \propto \exp[-(ka - ka_0)^2/4\alpha] \quad (3)$$

The time-domain solution for the particular a_0 is obtained from

$$P_s = \frac{1}{2\pi}\int_{-\infty}^{\infty}\exp[-i(ka)s]\,f(ka)g_i(ka)\,d(ka) \quad (4)$$

In general, we use one of the two forms for the g_i:

$$g_i(ka) = \begin{cases} 1 & \text{cw ping} \\ C\exp[-(ka - ka_0)^2/4\alpha] & \text{pulse} \end{cases} \quad (5)$$

Because of the phase-averaging effects in the nonresonance region, it is a good assumption that the only contributions in Eq. (5) occur at resonances. We then arrive at the expression

$$\int_{-\infty}^{\infty}\frac{-\left(\frac{1}{2}\right)\Gamma_n^{(r)}}{x - x_n^{(r)} - \left(\frac{1}{2}\right)\Gamma_n^{(r)}}\exp(-ixs)\,dx = \left(\frac{1}{2}\right)\Gamma_n^{(r)}\sin(x_n^{(r)}s)\exp\left[-\left(\frac{1}{2}\right)\Gamma_n^{(r)}s\right] \quad (6)$$

By summing the pole contributions, we arrive at the expression

$$p(s) = \sum_{n=m}^{N}\left(\frac{1}{2}\right)\Gamma_n^{(r)}\sin(x_n^{(r)}s)\exp\left[-\left(\frac{1}{2}\right)\Gamma_n^{(r)}s\right] \quad (7)$$

where the sum is over a nest of resonances. If we are in a frequency region where the resonance widths and spacings are approximately uniform, then

$$\Gamma_{n+1}^{(r)} \approx \Gamma_n^{(r)} \quad \text{and} \quad x_{n+1}^{(r)} - x_n^{(r)} \approx x_n^{(r)} - x_{n-1}^{(r)} \approx \Delta x^{(r)} \quad (8)$$

Then, by summing 2^M contributions from the nest, through some trigonometric manipulation, we obtain the important expression

$$P(s) \propto 2^M[\sin(x_{\text{avg}}^{(r)}s)]\,[\cos(\Delta x^{(r)}s/2)]^M\exp[-s\Gamma/2] \quad (9)$$

where

$$x_{\text{avg}}^{(r)} = \frac{1}{2N}\sum_{i=n}^{n+2N} x_i^{(r)}$$

which shows clearly the prominence of the carrier frequency, related to the phase velocity, and the existence of an envelope frequency, related to the group velocity as well as the exponential damping factor, which, as is expected, is known to be related to the half-width.

We can summarize the results indicated by Eq. (9) as follows:

1. The half-width is associated with the decay of the response in the time-domain solution: the response decreases exponentially with increasing value of the half-width. This is not altogether unexpected because narrow resonances are associated with long ringing times, and it is analogous to well-defined energies being associated with long half-lives in quantum physics.
2. The larger the number of adjacent resonances (2^M) sensed, the more sharply defined the return pulse or envelope function (the beats) and the more enhanced the return signal will be. Under appropriate conditions

we can get the group velocity of a specific type of resonance.

3. The larger the carrier frequency, the more oscillatory the signal within the envelope will be.
4. If several adjacent resonances sensed by a signal are different in character in the region of the carrier frequency, then it becomes difficult to interpret results in terms of a group velocity associated with a particular resonance type. Attempts at such interpretations could lead to erroneous results. For example, if one senses two resonances, one a Rayleigh resonance and one a whispering gallery resonance, the extraction of a group velocity associated with a specific type resonance would lead to error.

2.3 *Thickness Effects Caused by Internal Reflections from a Shell at High Frequency*

If one scatters a plane wave from an elastic shell at a frequency at which the interior wavelength (associated with the compressional velocity of the material) is equal to an integral value of the thickness, then it can be shown that the shell will appear transparent to the signal. Consequently, the signal will reflect off of the inner surface of the shell and add coherently with the specular signal at detection. For evacuated shells, this tends to produce a maximum at such values, and indeed, results that follow substantiate this. This maximum occurs at the critical frequency of the first symmetric Lamb mode S_1 in the shell. Although this result is not properly a "resonance" in the sense of the other processes discussed here, for want of a better term we will refer to this rather large response as a resonance. It can also be shown that the upper value of ka at which this process takes place for a given thickness and multiple of a half-integer terminates with the lowest partial wave allowed. Thus, an examination of the partial waves at the lowest mode can substantiate our interpretation of this phenomenon, which is illustrated in the last section.

3 Analysis of Results

In this section we analyze frequency- and time-domain scattering for five types of resonances. The first analysis pertains to Rayleigh- and Lamb-type resonances, mainly to contrast with the remaining results. We then examine flexural or bending resonances. Next, we analyze WC and steel shells at coincidence frequencies (frequencies at which the flexural phase velocity is equal to the speed of sound in the surrounding fluid) to verify the existence of waterborne resonances, first noted by Junger in the 1950s (see, for example, Ref. 15). These representative examples prove useful in exploiting expressions derived in the previous section for the time-domain case. The study is done both in the time and frequency domains because both cases have quite different resonance signatures. Finally, we examine thickness resonances from high-frequency incident plane waves on elastic shells. These "resonances," or rather internal reflections, occur when the wavelength caused by the compressional waves corresponds to a half-integral wavelength of the shell thickness. At that point, it can be shown that the shell is "transparent" to the incident wave and reflects from the inner surface (the core is assumed to be evacuated), which yields a maximum return signal.

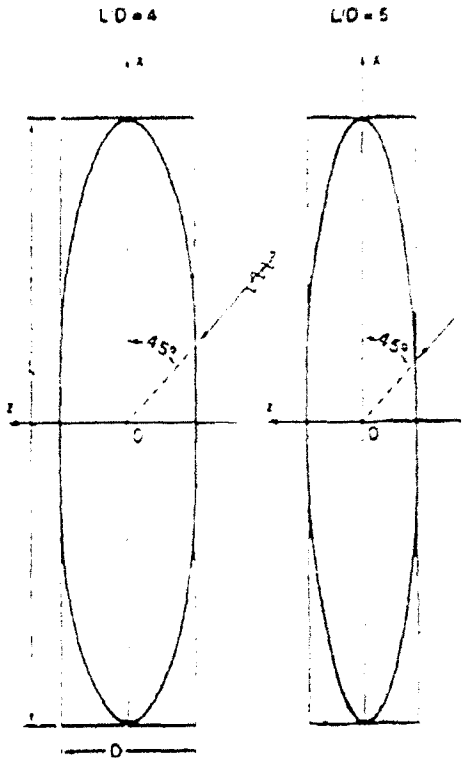

Fig. 1 Two of the prolate spheroids and their circumscribed beams.

3.1 *Rayleigh, Lamb, and Bending Resonances*

We now examine a phenomenon specific to elastic objects with smooth boundaries surrounded by an acoustic fluid, namely, body resonances. The body resonances examined originate from the curved-surface equivalents of seismic interface waves of pseudo-Rayleigh or Scholte type, propagating circumferentially to form standing waves on a bounded object. If phase velocities are slowly varying (as a function of frequency) at the object surface, resonances occur at discrete values of $kL/2$. These resonances manifest themselves in a prescribed manner (described below). For elongated elastic solids, three distinct resonance types occur. The first kind that we illustrate has to do with bending modes or flexural resonances. For unsupported spheroids, a plane incident wave at 45 deg relative to the axis of symmetry can excite the modes illustrated in Fig. 1 for aspect ratios of 4 and 5 to 1. It can be shown that the lowest mode corresponds to 2, and thereafter to 3, 4, etc. The interesting thing about these resonances is that they can be predicted by exact beam theories and coincide nicely with results given here. Of particular interest, is the effect that with increasing aspect ratio the onset of resonances occurs at lower $kL/2$ values; the opposite to the observed in Rayleigh resonances. The resonances predicted for aspect ratios of 3, 4, and 5 are illustrated in Figs. 2(a), 2(b), and 2(c). The modal pattern is illustrated in Fig. 3 for the first four modes. A comparison between the exact calculation (solid line) and resonances predicted by the Timosnenko beam theory (dashed line) is presented in Fig. 4 for aspect ratios of 1.5 to 5. The agreement between exact (T-matrix) solution and beam theory is seen to be quite good.

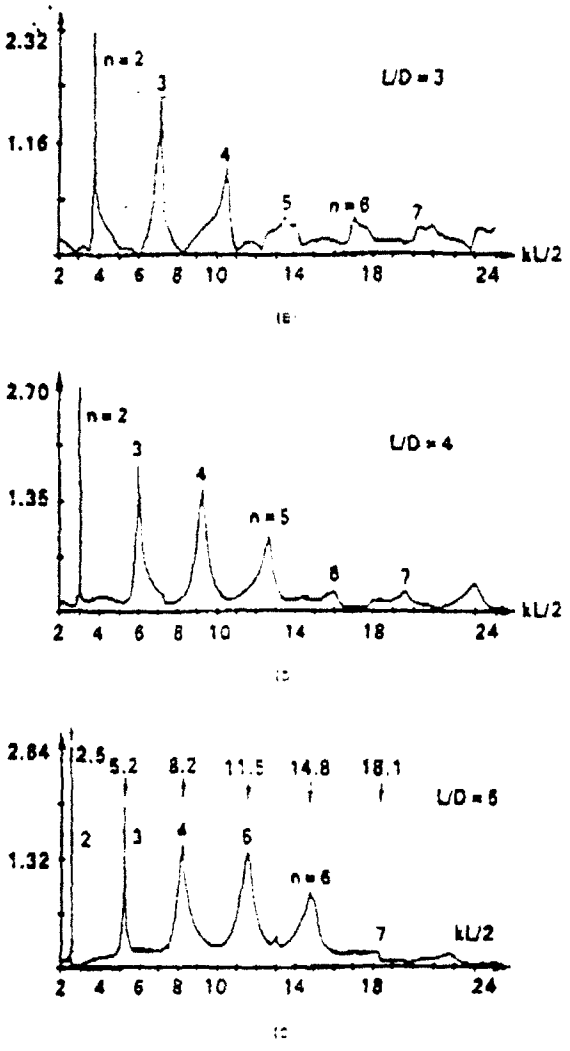

Fig. 2 Form functions for a steel spheroid in water at 45 deg: (a) aspect ratio of 3, (b) aspect ratio of 4, and (c) aspect ratio of 5

The second kind of resonances (at lower frequencies) are caused by leaky Rayleigh waves and have been shown to be related to both target geometry and material parameters (notably shear modulus and density). Resonances can, in this case, best be observed by examining the backscattered echo amplitude plotted as a function of $kL/2$, often referred to in the acoustic scattering literature as a *form function*. We illustrate this in Fig. 5 for broadside scattering from spheroids of aspect ratio 2, 3, 4, and 5. Here we see two resonances superimposed on the semiperiodic pattern caused by Franz waves associated with rigid scattering. If we subtract rigid scattering (in partial-wave space) from the elastic response, then we are left with the resonance response (see examples in Ref. 16). In addition to the above wave phenomena, it is also possible to excite whispering gallery resonances, which can be seen for the lowest aspect ratio cases in Fig. 5. In Fig. 5, the parallel sign indicates that the resonances are excited about the longest meridian, whereas the perpendicular sign indicates that the resonance is excited about the shortest meridian. The fact that broadside incident plane waves do excite resonances not only about the shortest

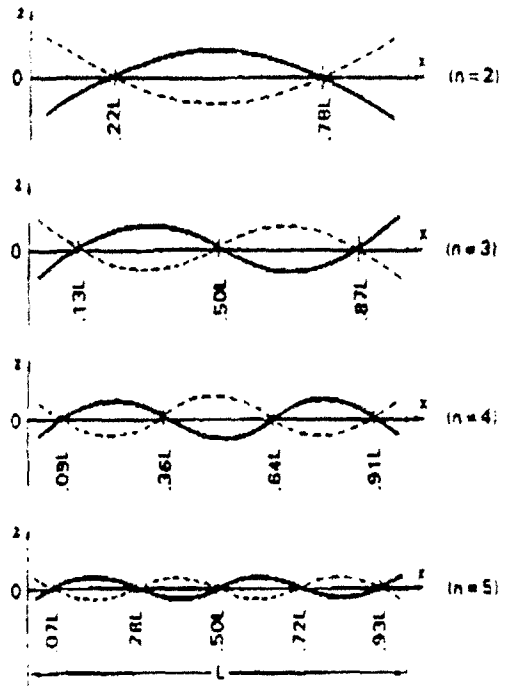

Fig. 3 First four vibrational modes of a free-free Timoshenko beam (TB).

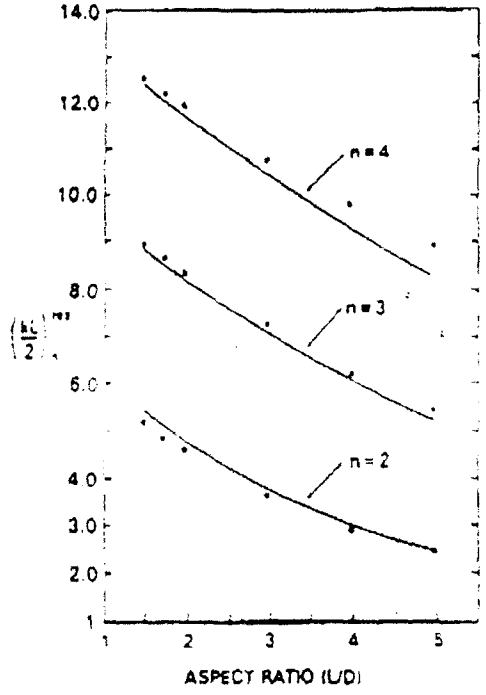

Fig. 4 Comparison of two models: solid line: *T* matrix and dots *Timoshenko beam theory.*

meridian but also about the longest meridian (coinciding with the resonances excited end-on) excludes the possibility that the resonances are caused by longitudinal "bar"-type waves. Finally, in Fig. 6, we examine scattering from a 1.5 to 1 aspect ratio aluminum shell at incidence angles of (a) end-on, (b) 45 deg relative to axis of symmetry, and (c)

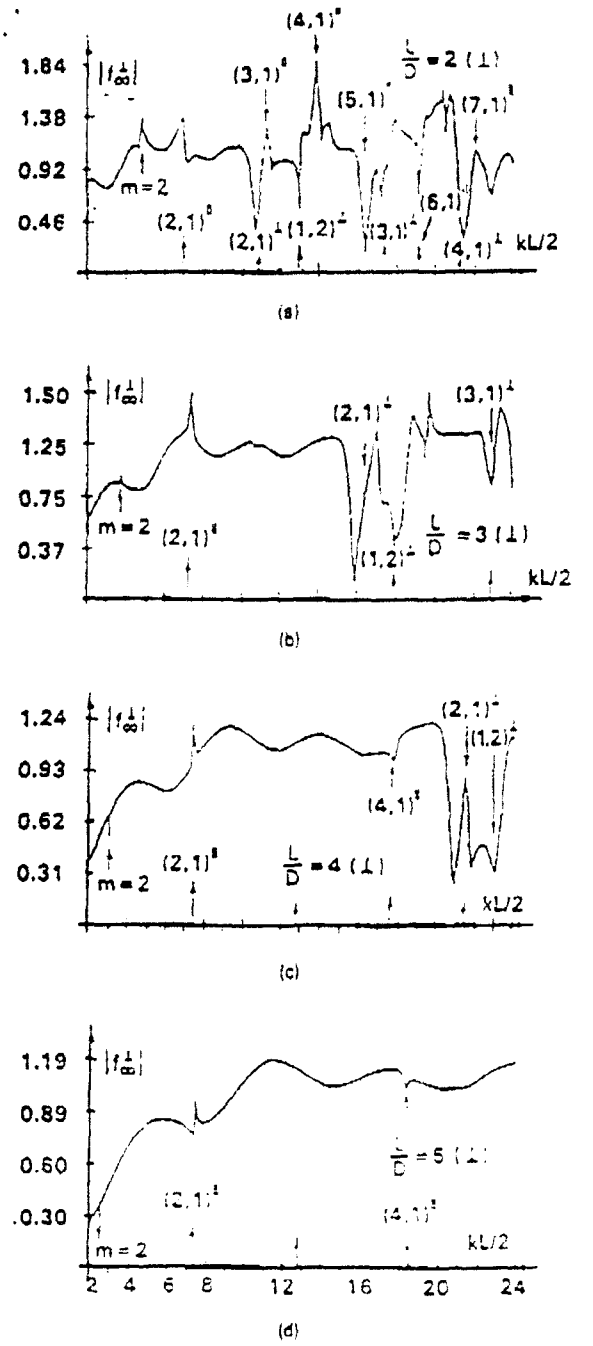

Fig. 5 Backscatter from solid steel spheroid at broadside incidence for aspect ratio of (a) 2 to 1, (b) 3 to 1, (c) 4 to 1, and (d) 5 to 1 for $kL/2 = 2$ to 24.[13]

broadside. Here we can excite three phenomena. At end-on, we observe the lowest symmetric Lamb resonances; at 45 deg we observe, in order of occurrence, a bending resonance, the lowest-order Lamb resonance excited about the largest meridian, and the two lowest Lamb modes excited about the smallest meridian. Additional bending resonances can be seen weakly at intermediate values. In Fig. 6(c) we see the broadside results in which the lowest bending mode is present as well as the lowest two Lamb modes about the

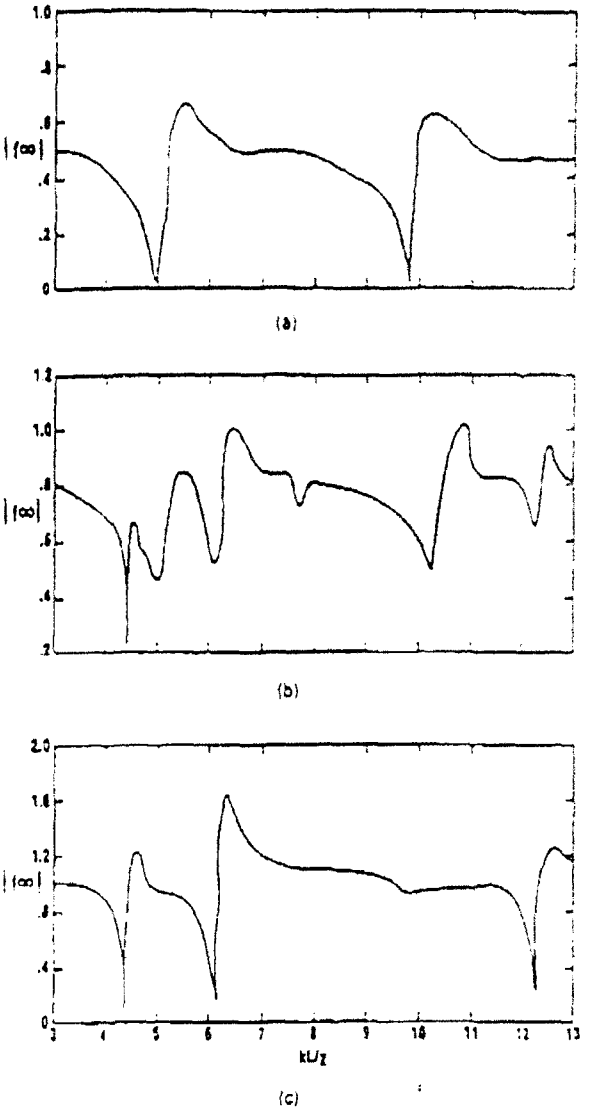

Fig. 6 Backscatter from a steel spheroid shell of aspect ratio of 1.5 for (a) end-on incidence, (b) 45 deg relative to the axis of symmetry, and (c) broadside incidence.[13]

shortest meridian. This means that with the exception of bending modes, an elastic shell (at least of this thickness) has resonances with only two degrees of freedom, and that both degrees can be excited at oblique angles (except at 90 deg) and that only the long (short) meridian types can be excited (end-on) broadside.

3.2 *Time-Domain Backscattering from Spherical Shells at Coincidence Resonance*

In contrast to symmetric Lamb waves, which yield resonances at low frequencies in a submerged shell, antisymmetric Lamb waves or flexural waves do not yield resonances until the phase velocity of the flexural wave is approximately equal to the speed of sound in the ambient fluid.[15] The frequency value for which this happens is referred to as the coincidence frequency. There are, however, subsonic fluid-borne waves that produce sharp[12-15] (fluid-

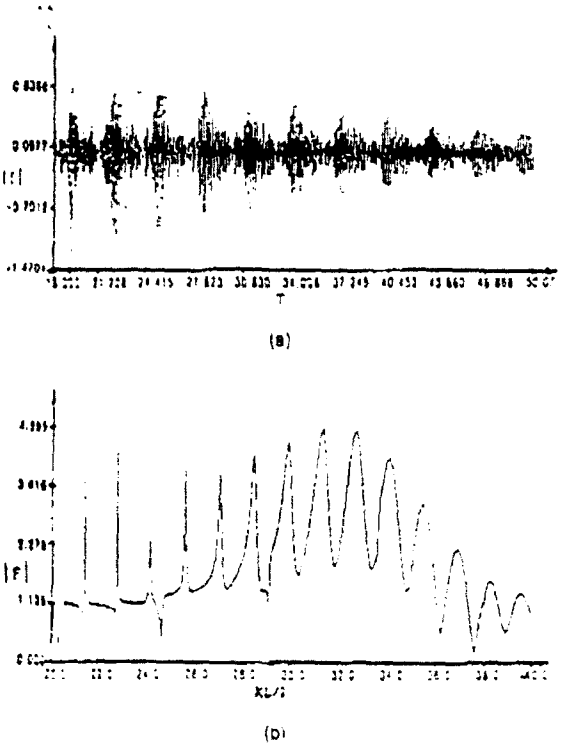

Fig. 7 (a) Time series—cw ping backscattered from 2.5% spherical WC shell in the time domain and (b) form function—backscattered echo from 2.5% WC shell in the frequency domain.

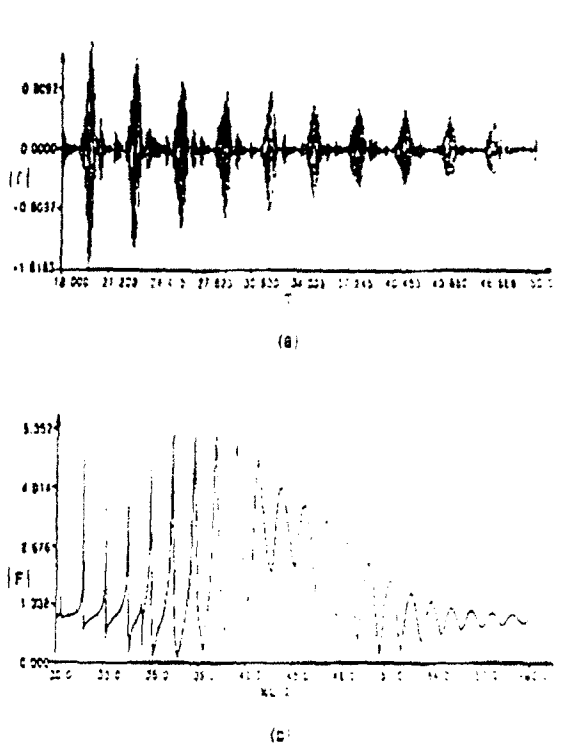

Fig. 8 (a) Time series—cw ping backscattered from 2.5% spherical steel shell and (b) form function—backscattered echo from 2.5% steel shell in the frequency domain.

borne) resonances below the coincidence frequency. We will refer to these fluid-borne waves as pseudo-Stoneley waves and the related resonances pseudo-Stoneley resonances.[31-33] The pseudo-Stoneley resonances are well defined in partial wave space, usually corresponding to only one partial wave mode number and to a very narrow half-width with a dispersive phase velocity that approaches the speed of sound in the fluid with increasing frequency. They diminish in significance at the point for which the flexural resonances begin to dominate. It has been observed that for both flat plates that are fluid loaded on one side and for submerged shells, at coincidence, one observes a very strong response. The associated resonance region has been referred to as the strong flexural region in the literature and can be interpreted[15] in terms of a singularity that occurs when the wave number in the fluid is equal to that of the flexural wave on the surface of the object. The strong effect at the coincidence frequency can be seen in Figs. 7(b) and 8(b), which illustrates the effect at the indicated *ka* range for a WC shell of 2.5% and a steel shell also at 2.5% thickness. Figure 9 illustrates the fact that pairs of partial waves are important at coincidence frequency, in which the broad contribution is related to the flexural wave and the narrow (slower) partial wave is related to the waterborne wave. Figures 9(a), 9(b), and 9(c) are the partial wave amplitudes for *ka* values of 33, 40, and 50. It is apparent that at the lower *ka*, the flexural mode is weak, whereas the waterborne mode, which is dispersive and at this point subsonic, is narrow and significant. Figure 9(b) is calculated at $ka = 40$, which illustrates that the flexural mode is becoming more dominant and well defined, and that the rather dispersive waterborne mode is approaching the speed of sound in water and is still dominant. At the point at which the flexural and waterborne waves have phase velocities that coincide, they seem to merge as illustrated in Fig. 9(c). Actually, what is happening is that the partial waves are overlapping, but actually they are somewhat out of phase so that at that point the actual form function has begun to get smaller. Shortly above this point the waterborne wave disappears. Note that at the coincidence frequency there is a phase change in the partial wave contributions as well, which accounts for the envelope of the resonance curve at coincidence (shown here and in subsequent plots) where the waves are in phase until coincidence and out of phase afterward. Our interest here is in examining the time-domain response because we expect the conditions of Eq. (8) to be partially met over a broad frequency range and thus to yield a strong coherent response with a carrier frequency in the neighborhood of the frequency at coincidence. Accordingly, we examine the case of cw pings for two examples for which one expects coincidence resonances to arise. This is certainly suggested by the strong responses in Figs. 7(b) and 8(b) at the *ka* values 32 and 45, respectively, for WC and steel. Further, we use the Mindlin-Timoshenko thick plate theory to determine the value for which the flexural phase velocity will equal the ambient speed of sound in water. The expressions we use are from flat plate theory, but they prove to be quite reliable in predicting the phase velocity for spherical shells near the coincidence frequency. It is remarkable that they, in fact, do predict the frequency range in the figures that match the peaks in the strong flexural region. We determine that the expression for the phase velocity is

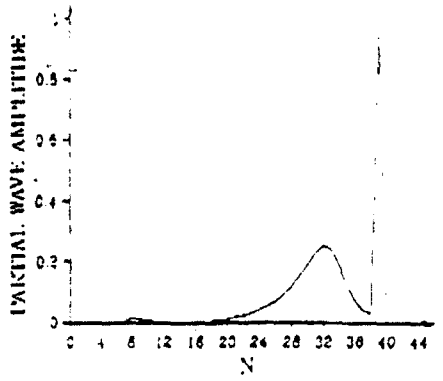

(a)

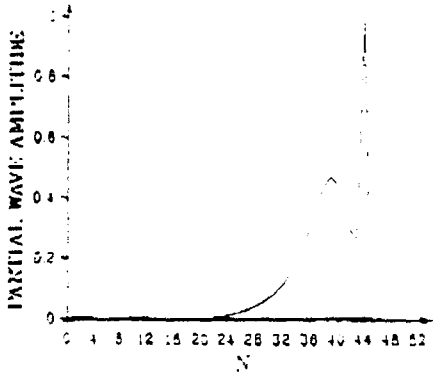

(b)

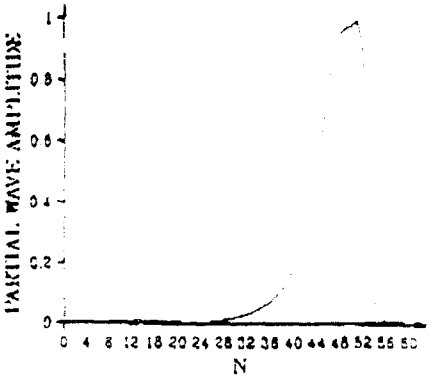

(c)

Fig. 9 Partial wave amplitudes for the steel example at (a) $ka = 33$, (b) $ka = 40$, and (c) $ka = 51$, as functions of the partial wave index n

$$v_f = \frac{c_p\left\{\left[(\Gamma-1)^2\left(\frac{\omega}{\Omega}\right)^4 + 4\left(\frac{\omega}{\Omega}\right)^2\right]^{1/2} - (\Gamma+1)\left(\frac{\omega}{\Omega}\right)^2\right\}^{1/2}}{\left\{2\left[1-\Gamma\left(\frac{\omega}{\Omega}\right)^2\right]\right\}^{1/2}} \tag{10}$$

where

$$\Omega = \frac{c_p\sqrt{12}}{a},$$

$$\Gamma = 2.65(1 - 1.5\nu - 0.75\nu^2),$$

$$\frac{\omega}{\Omega} = \frac{(ka)c_w\left(\frac{h}{a}\right)}{c_p\sqrt{12}},$$

$$c_p = c_t\left(\frac{2}{1-\nu}\right)^{1/2}$$

Here c_t is the shear speed and ν is the Poisson ratio of the material. The ratio h/a is a thickness parameter and c_w is the speed of sound in water. The remaining defining expressions in Eq. (10) are discussed in Ref. 11. For the cases presented here, h/a is 0.025, where a is the radius of the sphere. The group velocity is determined by us to be

$$\frac{d\omega}{dk} = \frac{\left[2c_p^2 - (\Gamma-1)v_f^2\right]\left(\frac{\omega}{\Omega}\right)^2}{12v_f^3c_p^2 - \left[(\Gamma-1)c_p^2v_f - 2\Gamma v_f^3\right]\left(\frac{\omega}{\Omega}\right)^2} \tag{11}$$

The expression predicts the point of coincidence quite nicely.

We now examine the time-domain calculations. For the first example, we examine tungsten carbide (WC) of 2.5% thickness, illustrated in Fig. 7(a). In this case, we observe a well-defined envelope with pronounced oscillations within the envelope consistent with expressions in the previous section. The enhancement caused by the factor 2^M is obvious both here and in Fig. 8(a). We can obtain the group velocity from the peak-to-peak distance. The result leads to a value of 2.23 km/s. The expression for flexural waves predicts a value of 2.53 km/s at coincidence and a range of 2.44 to 2.68 km/s over the ka range of 25 to 50, where the strong flexurals are significant. In that range, the phase velocity ranges from 1.37 to 1.58 km/s. The values of the predicted and extracted group velocities are not in extremely good agreement; the disagreement is about 12%. This may be caused in part by the fact that flat plate theory may be in error or inadequate for spherical fluid-loaded targets. We have determined the group velocity of the pseudo-Stoneley wave for this case to be 2.65 km/s, based on plate theory. Moreover, the phase velocity is in the range from 88 to 98% of the speed of sound in the fluid. This value of group velocity is within 3% of the extracted value from the time-domain solution. Moreover the pseudo-Stoneley resonances have very narrow widths, whereas the flexural resonances are quite broad. The conditions in Sec. 2 would indicate that the flexural resonances would rapidly dampen whereas the pseudo-Stoneley resonances would attenuate slowly. Thus, based on the similarity of the extracted group velocity to that of the pseudo-Stoneley wave and the conditions in Sec. 2 we conclude that the time-domain calculations in Fig. 7(a) represent pseudo-Stoneley resonances.

The final example is for the steel shell of 2.5% thickness. The results here are consistent with that of the steel case and are illustrated in Fig. 8(a). Here the group velocity was

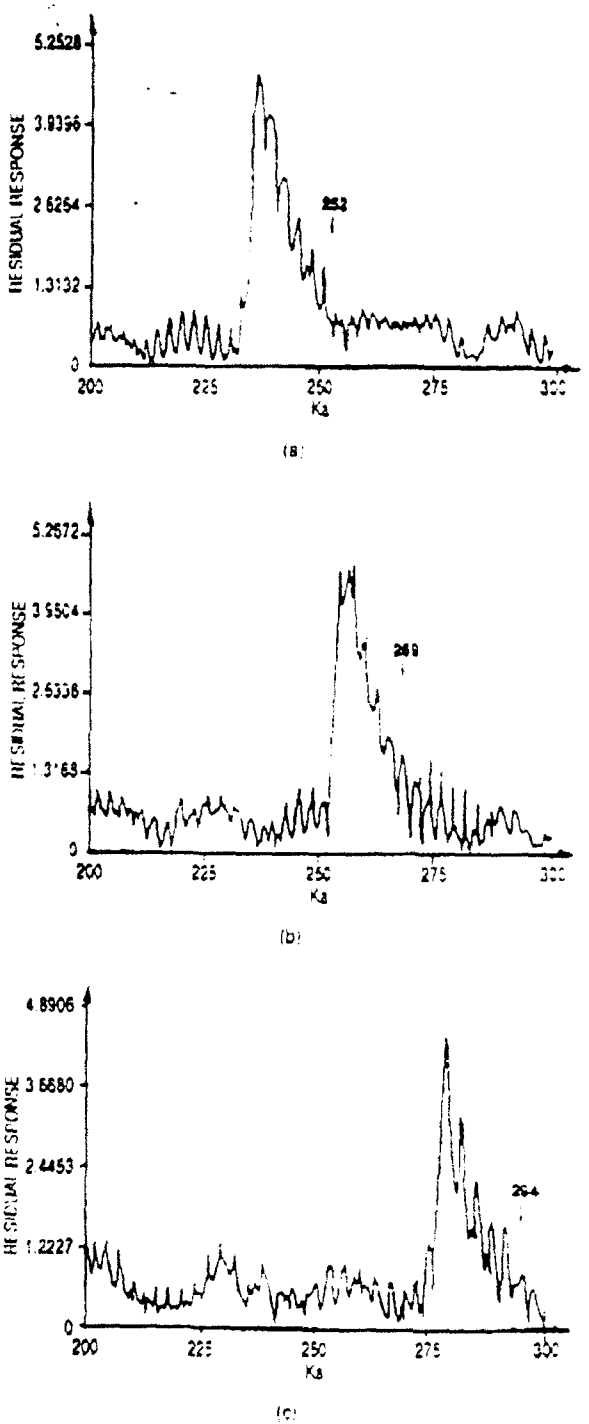

Fig. 10 Residual response for an $h/a = 5\%$ thick shell displaying the thickness resonance: (a) steel shell, (b) molybdenum shell, and (c) WC shell.

extracted to be 2.16 km/s as opposed to the plate theory value of 2.33 km/s for flexural waves. The range of values for the group velocities predicted from the flat plate theory was from 2.49 to 2.78 km/s over the ka range of 40 to 60. Here again, the difference was 12% between plate theory and the extracted value. On the other hand, the group velocity for pseudo-Stoneley waves is 2.26 km/s, which is within 3% of the extracted value. As in the previous example, the pseudo-Stoneley resonances are quite narrow, whereas the flexural resonances are broad, and we conclude that the results of Fig. 8(a) represent predominantly pseudo-Stoneley resonances.

3.3 *Thickness "Resonances" in the Echoes Returned by Elastic Shells at High Frequency*

Figures 10(a), 10(b), and 10(c) are the form functions caused by a plane wave incident on spherical shells for 5% steel, molybdenum, and WC, respectively. It is evident that in the region between about $ka = 240$, 265, and 290 there are rather pronounced returns that are quite a bit larger in amplitude than usually observed for symmetric and antisymmetric resonances. The explanation for this event is determined from the fact that when a wave goes into a layered material, if the dilatational wavelength of the layer is equal to half the wavelength of the penetrating wave, then the reflection coefficient is just equal to that caused by the interior layers, which in this case corresponds to a soft scatterer (i.e., the cavity was evacuated), and thus, the reflected signal when added to the usual surface reflected signal is at a maximum. To determine where this happens we examine at what value of ka this will happen for a steel shell with compressional speed 5.95 km/s. The pertinent relation from a flat plate approximation (adequate at high frequency) is

$$ka = \frac{n\pi c_d}{(h/a)c_w} \qquad n = 1, 2, 3, \ldots \tag{12}$$

Here c_d and c_w are the speeds of compressional waves for steel and water, respectively (5.95 km/s and 1.4825 km/s), and h/a is the ratio of the thickness to the radius of the shell (here 0.1, 0.025, and 0.05). Thus $ka = 126$, 252, and 504, respectively, which are in the range of the large returns. Figures 11(a) and 11(b) are the form functions of steel shells of 10% and 2.5%, respectively. The compressional velocities of molybdenum and WC are 6.35 and 6.95, which predict in the correct range. To determine that this is indeed the correct interpretation we examine where the plot is a maximum for the zero-order partial wave corresponding best to the flat plate approximation. Figures 12(a), 12(b), and 12(c) illustrate that this, indeed, is at $ka = 126$, 252, and 504, respectively, for the steel cases. Moreover, Figs. 13(a) and 13(b) for the lowest partial waves of the cases in Figs. 10(b) and 10(c) yield similar agreement. The broad width of the resonances is due to the fact that the thickness at which the plane incident wave "sees" the shell is usually greater than the shell thickness, and must correspond to higher order partial waves but lower ka values. This interpretation also predicts higher-order resonances (when the thickness is equal to a multiple of half-integer compressional wavelengths), and indeed the predictions are corroborated and will be illustrated elsewhere.

4 Conclusions

We have illustrated several new large resonance patterns that offer a means of target identification. Dolphins are known to be able to distinguish between coins of different material; perhaps they make use of the thickness resonance. At the lower frequency end, time-domain signals centered

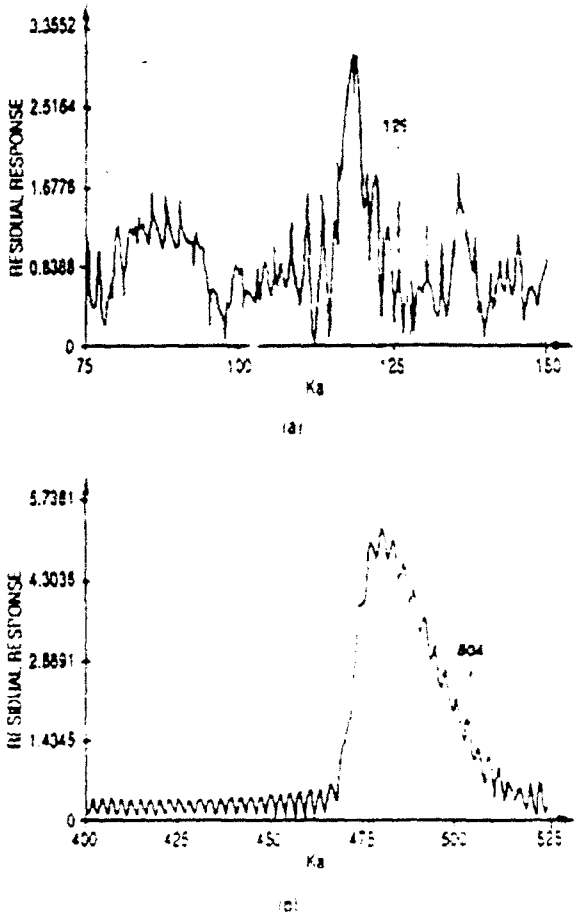

Fig. 11 Residual response for (a) 10% and (b) 2.5% steel shell showing the thickness resonance.

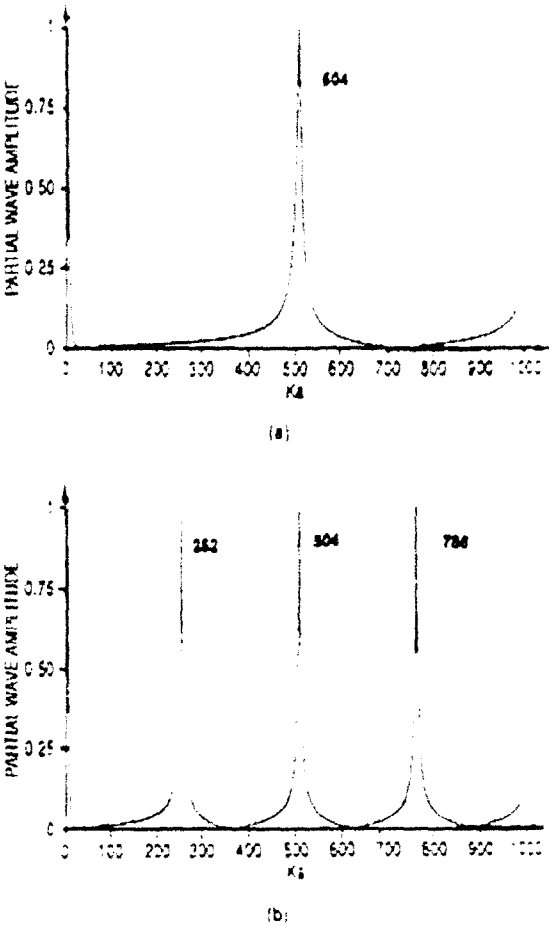

Fig. 12 Lowest partial wave amplitudes for (a) 2.5%, (b) 5%, and (c) 10% steel shell up to $ka = 1000$

about the coincidence frequency are likely to be a useful tool for some considerations. The resonances caused by bending modes are rather narrow, which may be difficult to detect in the frequency domain but showed some promise when using the methods in the time domain along with gating techniques.

Acknowledgments

The authors gratefully acknowledge the support received from the Independent Research Program of the Naval Surface Warfare Center and from the Core Research Program at the Naval Oceanographic and Atmospheric Research Laboratory.

References

1. P. C. Waterman, "New formulation of acoustic scattering," *J. Acoust. Soc. Am.* 45, 1417 (1969).
2. P. C. Waterman, "Matrix formulation of electromagnetic scattering," *Proc. IEEE* 53(3), 805 (1965).
3. P. C. Waterman, "Matrix theory of elastic wave scattering II: a new conservation law," *J. Acoust. Soc. Am.* 63(6), 1320 (1977).
4. M. F. Werby and S. Chin-Bing, "Numerical techniques and their use in extension of T-matrix and null-field approaches to scattering," *Int. J. Comp. Math. Appls.* 11(7/8), 717 (1985).
5. M. F. Werby, G. Tango and L. H. Green, "Eigenvalue and similarity transformation methods in the solution of acoustical scattering problems," in *Computational Acoustics: Algorithms and Applications*, Vol. 2, pp. 257–278, D. Lee, R. L. Sternberg, and M. H. Schultz, Eds., Elsevier Science Publishers, The Netherlands (1988).
6. Y.-H. Pao and V. Varatharajulu, "Huygens's principle, radiation conditions, and integral formulas for the scattering of elastic waves," *J. Acoust. Soc. Am.* 60(7), 1361 (1976).
7. A. Boström, "Scattering of stationary acoustic waves by an elastic obstacle immersed in a fluid," *J. Acoust. Soc. Am.* 67(2), 390 (1980).
8. B. A. Peterson, V. V. Varadan, and V. K. Varadan, "T-matrix approach of study of vibrational frequencies of elastic bodies in fluids," *J. Acoust. Soc. Am.* 74(5), 1051 (1983).

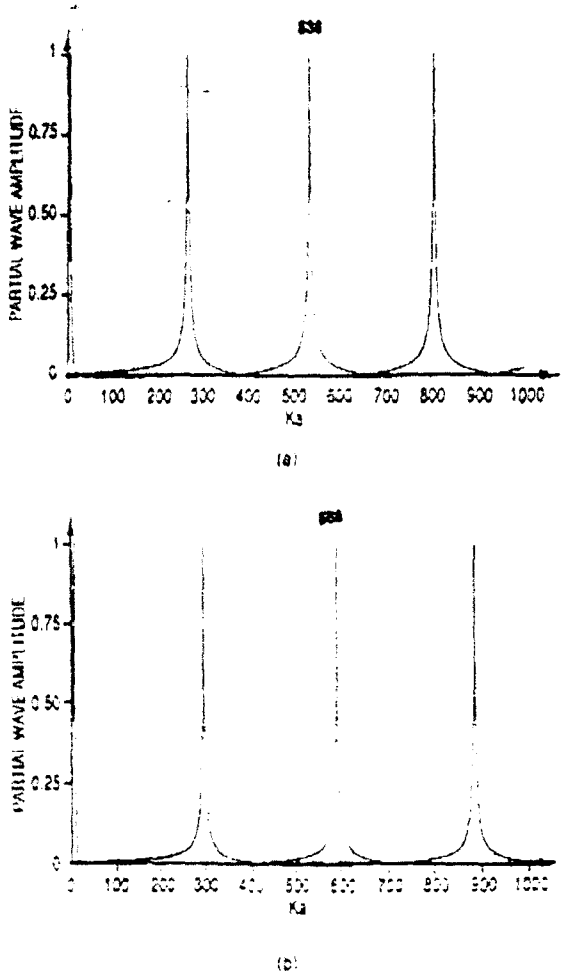

Fig. 15 Lowest partial wave amplitudes for a 5% (a) molybdenum shell and (b) WC shell up to $ka = 1000$

9. M. F. Werby and L. R. Green, "An extended unitary approach for acoustical scattering from elastic shells immersed in fluids," *J. Acoust. Soc. Am.* 74(2), 625–632 (1983).
10. M. F. Werby and G. Gaunaurd, "Classification of resonances from scattering at arbitrary incident angles from submerged spheroidal shells," *J. Acoust. Soc. Am.* 82, 1369–1379 (1987).
11. M. F. Werby and G. G. Gaunaurd, "Flexural resonances in obliquely insonified solid elastic spheroids," *J. Acoust. Soc. Am.* 85, 2365–2371 (1989).
12. H. Überall, "Modal and surface-wave resonances in acoustic-wave scattering from elastic objects and in elastic-wave scattering from cavities," in *Proc. IUTAM Symp.: Modern Problems in Elastic Wave Propagation*, J. Miklowitz and J. D. Achenbach, Eds., Wiley Interscience, p. 239 (1978). G. Gaunaurd, "Resonant theory of elastic and viscoelastic wave-scattering and its application to the spherical cavity in absorptive media," *Proc.* same p. 550. G. C. Gaunaurd and H. Überall, "Theory of resonance scattering from spherical cavities in elastic and viscoelastic media," *J. Acoust. Soc. Am.* 63, 1699–1712 (1978). G. Gaunaurd, "Elastic and acoustic resonance wave-scattering," *Appl. Mech. Rev.* 42, 143–192 (1989); and, G. Gaunaurd and M. F. Werby, "Acoustic resonance scattering by submerged elastic shells," *Appl. Mech. Rev.* 43, 171–208 (1990).
13. M. Werby and G. Gaunaurd, "Broadside resonance scattering from elastic spheroids," *IEEE J. Oceanic Eng.* OE-14, 400–406 (1989).
14. M. F. Werby and G. C. Gaunaurd, "Transition from soft to rigid behavior in scattering from submerged thin elastic shells," *Acoust. Lett.* 9(7), 89–93 (1986).
15. M. C. Junger and D. Feit, *Sound Structures and their Interaction*, MIT Press, Cambridge, Mass. (1972).
16. C. Dean and M. F. Werby, "Target shape and material composition from the resonance echoes of submerged elongated elastic targets," in Automatic Object Recognition, *Proc. SPIE* 1471 (1991).
17. J. George and M. F. Werby, "Study and characterization of 3-dimensional angular distributions of rigid, soft, and elastic spheroidal targets," *Proc. SPIE* 1471 (1991).
18. M. F. Werby and H. B. Ali, "Time domain solution from the frequency domain: application to resonance scattering from elastic bodies," in *Computational Acoustics* Vol. 2, pp. 133–148, D. Lee, A. Cakmak, and R. Vichnevetsky, Eds., Elsevier Science Publications, The Netherlands (1990).
19. E. McDaid and G. C. Gaunaurd, "Signal processing of ideal echoes resonantly scattered by underwater structures," *J. Acoust. Soc. Am.* **88**, 2720–2735 (1990).
20. G. Gaunaurd and W. Wertman, "Transient acoustic scattering by submerged elastic shells," *Int. J. Solids Structures* 27, 699–711 (1991).
21. G. Gaunaurd and M. Werby, "Sound scattering by resonantly excited fluid-loaded, elastic spherical shells," *J. Acoust. Soc. Am.* 90, 2536–2557 (1991).
22. M. Talmant, H. Überall, R. D. Miller, M. F. Werby, and J. W. Dickey, "Lamb waves and fluid borne waves on water-loaded, air-filled thin spherical shells," *J. Acoust. Soc. Am.* 86, 278–289 (1989).
23. G. Quentin and M. Talmant, "The Plane Plate Model Applied to Scattering of Ultrasonic Waves from Cylindrical Shells," in *Proc. Int. Conf. on Elastic Wave Propagation*, M. F. McCarthy and M. A. Hayes, Eds., Elsevier Publications, The Netherlands (1989).

Michael F. Werby: Biography and photograph not available.

Guillermo C. Gaunaurd received his PhD in physics/acoustics from Catholic University, Washington, D.C., in 1971. He has been a research physicist in the Research Department of the Naval Surface Warfare Center, White Oak, Maryland, since 1971 specializing in acoustics and electromagnetic radiation and scattering. He is currently a group leader in the Physics and Technology Division of that institution where he carries on a research program on the basic interaction of waves with materials. He has been a lecturer at the University of Maryland since 1984. He has authored over 100 journal articles and is a member of many professional and honor societies. He is a senior member of the IEEE and a fellow of the Acoustical Society of America and of the Washington Academy of Sciences. His professional biography appears in Marquis *Who's Who in America* and a dozen other similar books. He is currently an associate editor for the IEEE *Journal of Ultrasonics, Ferroelectrics and Frequency Control*.